The Long-Wavelength Macromolecular Crystallography Beamline I23 at Diamond Light Source

Armin Wagner
Diamond Light Source

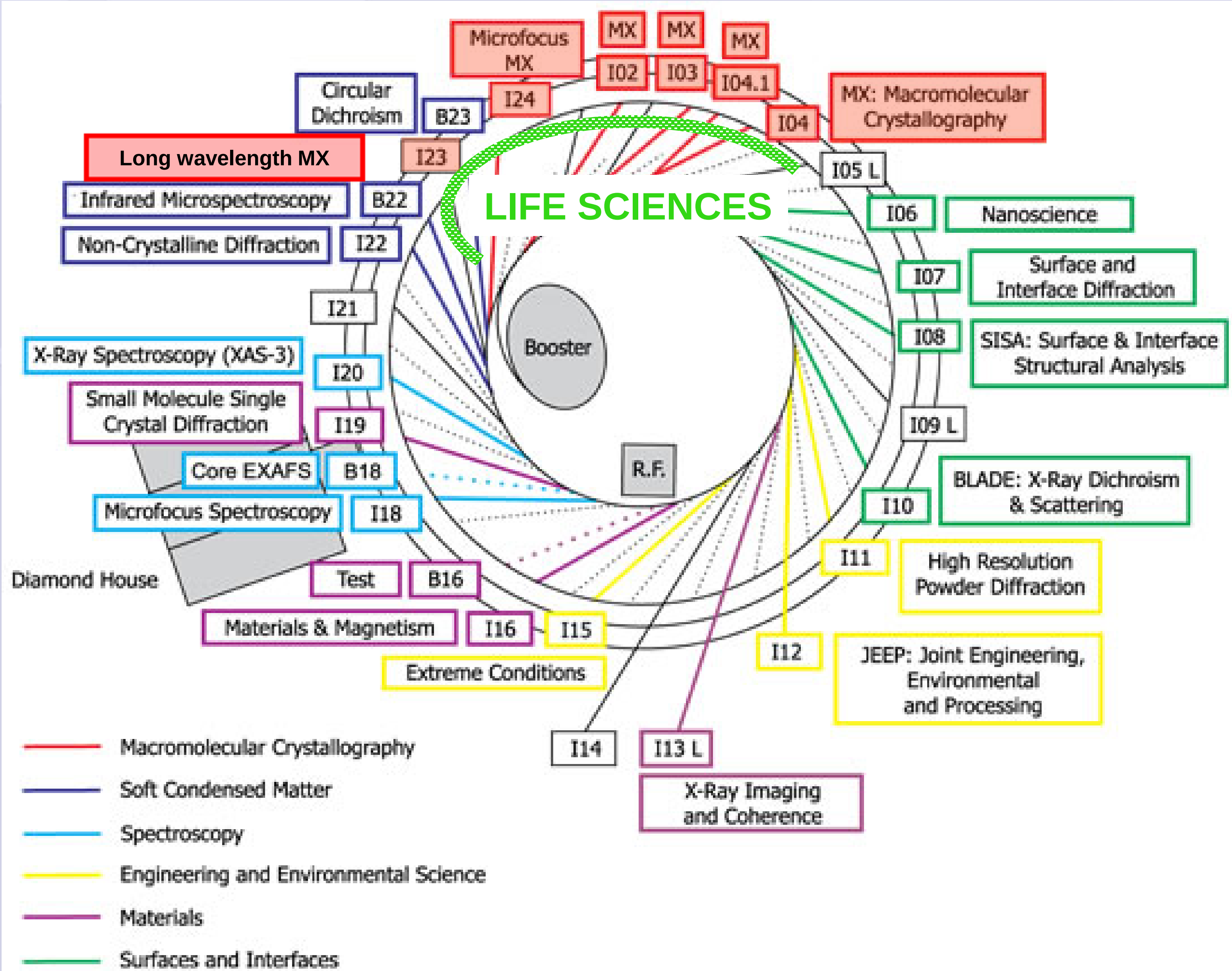
Microfocus MX
MX
MX
MX
I102
I103
I104.1
Circular Dichroism
B23
I24
MX: Macromolecular Crystallography
I04
Long wavelength MX
I23
I05 L
Infrared Microspectroscopy
B22
LIFE SCIENCES
I06
Nanoscience
Non-Crystalline Diffraction
I22
I07
Surface and Interface Diffraction
I21
Booster
I08
SISA: Surface & Interface Structural Analysis
X-Ray Spectroscopy (XAS-3)
I20
Small Molecule Single Crystal Diffraction
I19
I09 L
Core EXAFS
B18
R.F.
BLADE: X-Ray Dichroism & Scattering
Microfocus Spectroscopy
I18
I10
I11
High Resolution Powder Diffraction
Diamond House
Test
B16
Materials & Magnetism
I16
I15
I12
JEEP: Joint Engineering, Environmental and Processing
Extreme Conditions
I14
I13 L
X-Ray Imaging and Coherence
Macromolecular Crystallography
Soft Condensed Matter
Spectroscopy
Engineering and Environmental Science
Materials
Surfaces and Interfaces

Why long wavelengths?

- Experimental Phasing
  - SAD phasing from native proteins and DNA by using anomalous signal from sulphur and phosphorous.
  - SAD and MAD phasing for large complexes by using enormous anomalous signals from M-edges.
- Element specific analysis

Acta Crystallographica Section D
Biological
Crystallography
ISSN 0907-4449

On the routine use of soft X-rays in macromolecular crystallography. Part III. The optimal data-collection wavelength

Christoph Mueller-Dieckmann, Santosh Panjikar, Paul A. Tucker and Manfred S. Weiss*

EMBL Hamburg Outstation, c/o DESY, Notkestrasse 85, D-22603 Hamburg, Germany

Correspondence e-mail: msweiss@embl-hamburg.de

Complete and highly redundant data sets were collected at different wavelengths between 0.80 and 2.65 Å for a total of ten different protein and DNA model systems. The magnitude of the anomalous signal-to-noise ratio as assessed by the quotient $R_{anom}/R_{r.i.m.}$ was found to be influenced by the data-collection wavelength and the nature of the anomalously scattering substructure. By utilizing simple empirical correlations, for instance between the estimated $\Delta F/F$ and the expected R_{anom} or the data-collection wavelength and the expected $R_{r.i.m.}$, the wavelength at which the highest anomalous signal-to-noise ratio can be expected could be estimated even before the experiment. Almost independent of the nature of the anomalously scattering substructure and provided that no elemental X-ray absorption edge is nearby, this optimal wavelength is 2.1 Å.

Received 6 April 2005
Accepted 5 July 2005

PDB References: ConA-Xe, 2a7a, r2a7asf; adaptin-Xe, 2a7b, r2a7bsf; PPE-Xe, 2a7c, r2a7csf; HEL-Xe, 2a7d, r2a7dsf; DNA, 2a7e, r2a7esf; HEL, 2a7f, r2a7fsf; thermolysin, 2a7g, r2a7gsf; trypsin, 2a7h, r2a7hsf; thaumatin, 2a7i, r2a7isf; PPE-Ca, 2a7j, r2a7jsf.

diamond

Optimal wavelength

- Radiation damage proportional to absorbed dose

$$I_E \propto \frac{t^3 e^{-\mu t}}{1-e^{-\mu t}} \lambda^3$$

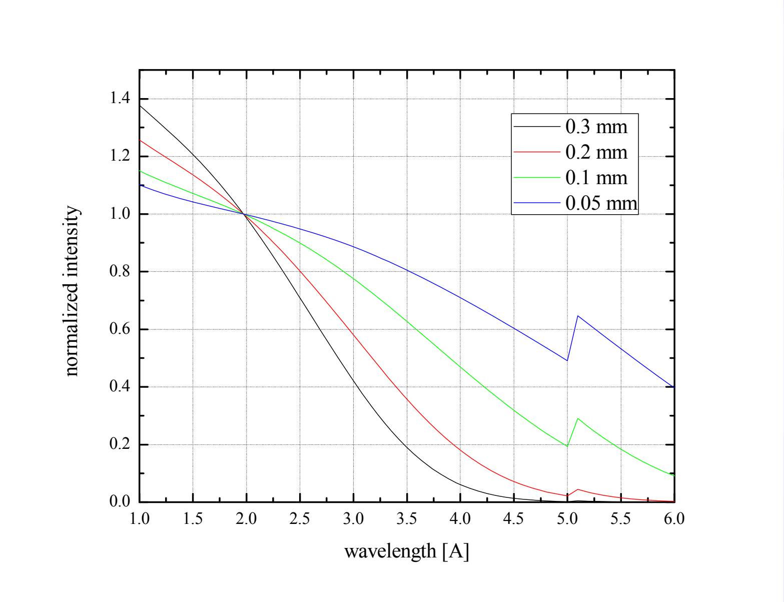

- Arndt (1984)
- Isometric crystal
- Bragg intensity per energy absorbed
- Radiation damage wavelength independent

J. Appl. Cryst. (1984). **17**, 118–119

Optimum X-ray wavelength for protein crystallography. By U. W. Arndt, *MRC Laboratory of Molecular Biology, Hills Road, Cambridge CB2 2QH, England*

diamond

Optimal wavelength for S-SAD

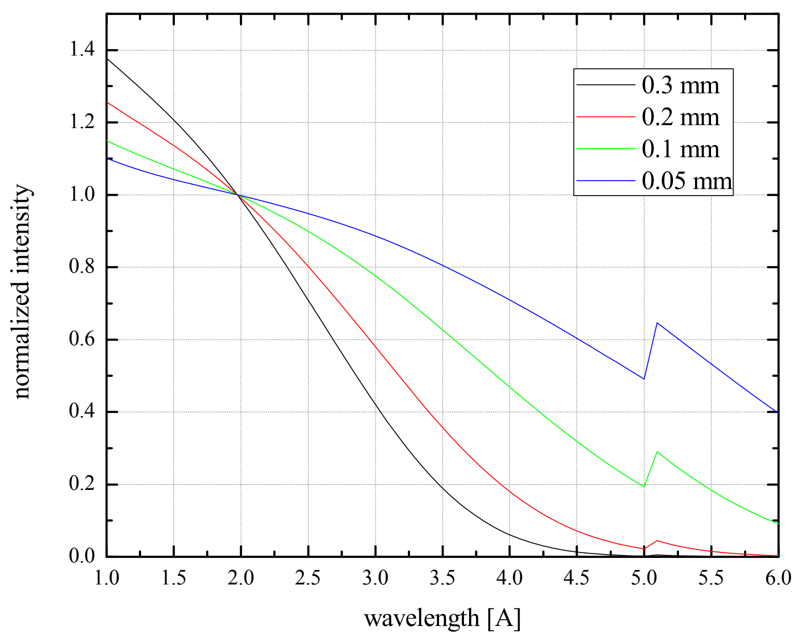

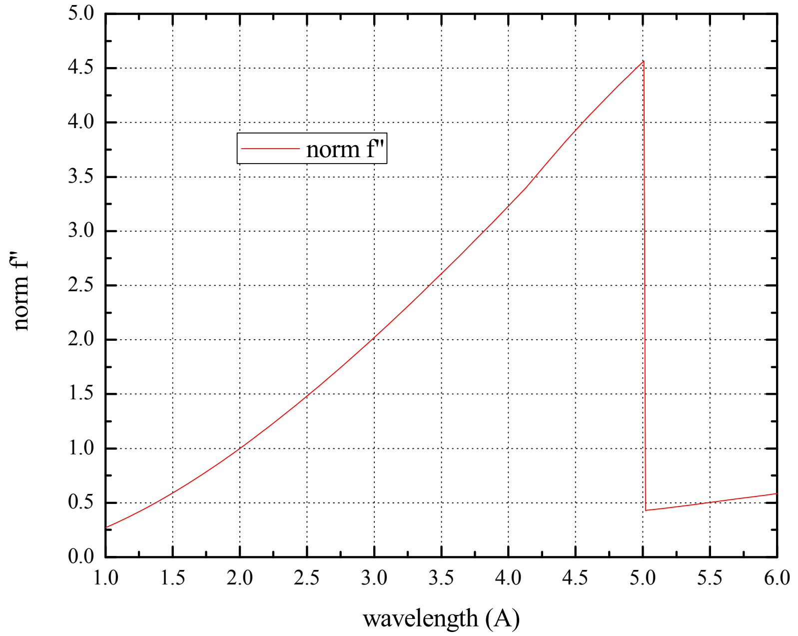

Optimal wavelength for S-SAD

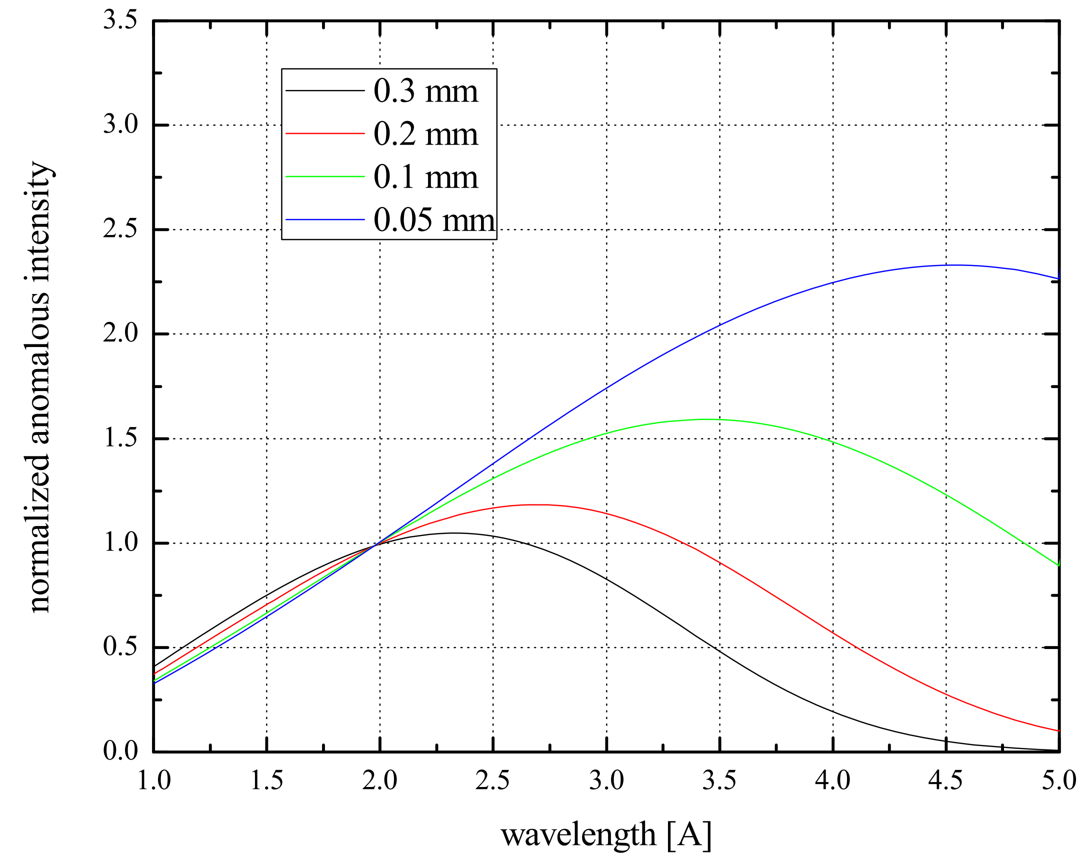

diamond

BUT!!!

ABSORPTION

DETECTORS

diamond

Air absorption

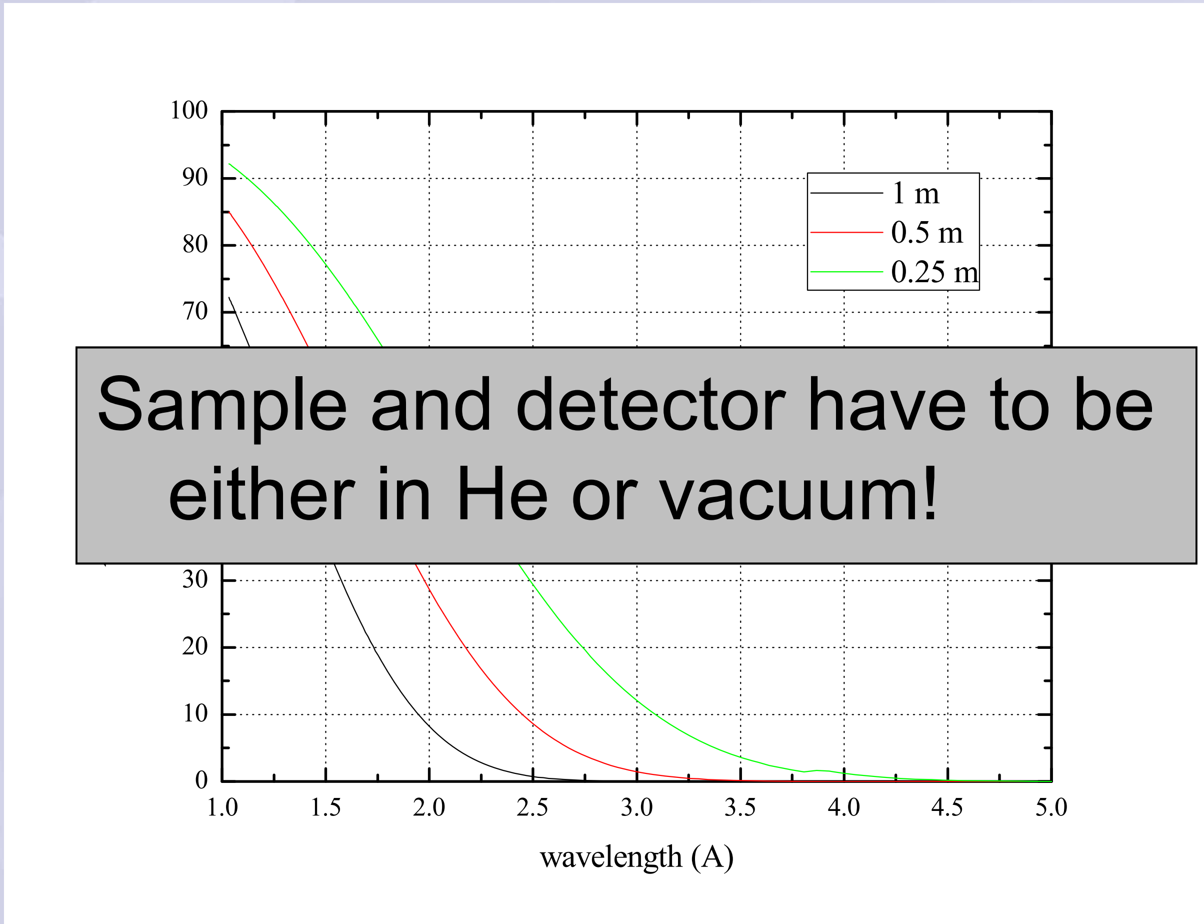

Sample and detector have to be either in He or vacuum!

Sample absorption

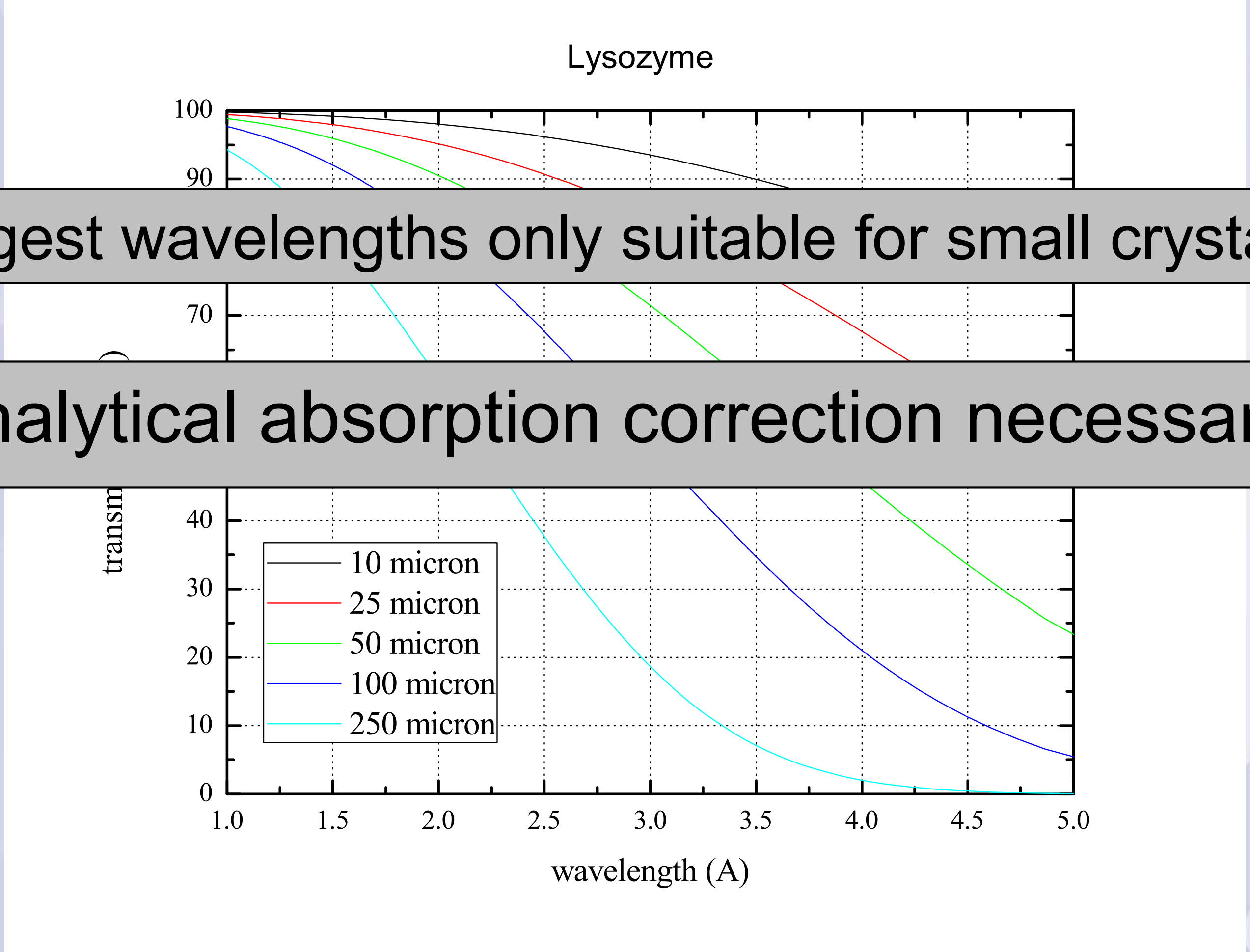

Longest wavelengths only suitable for small crystals!

Analytical absorption correction necessary!

Solvent and loop absorption

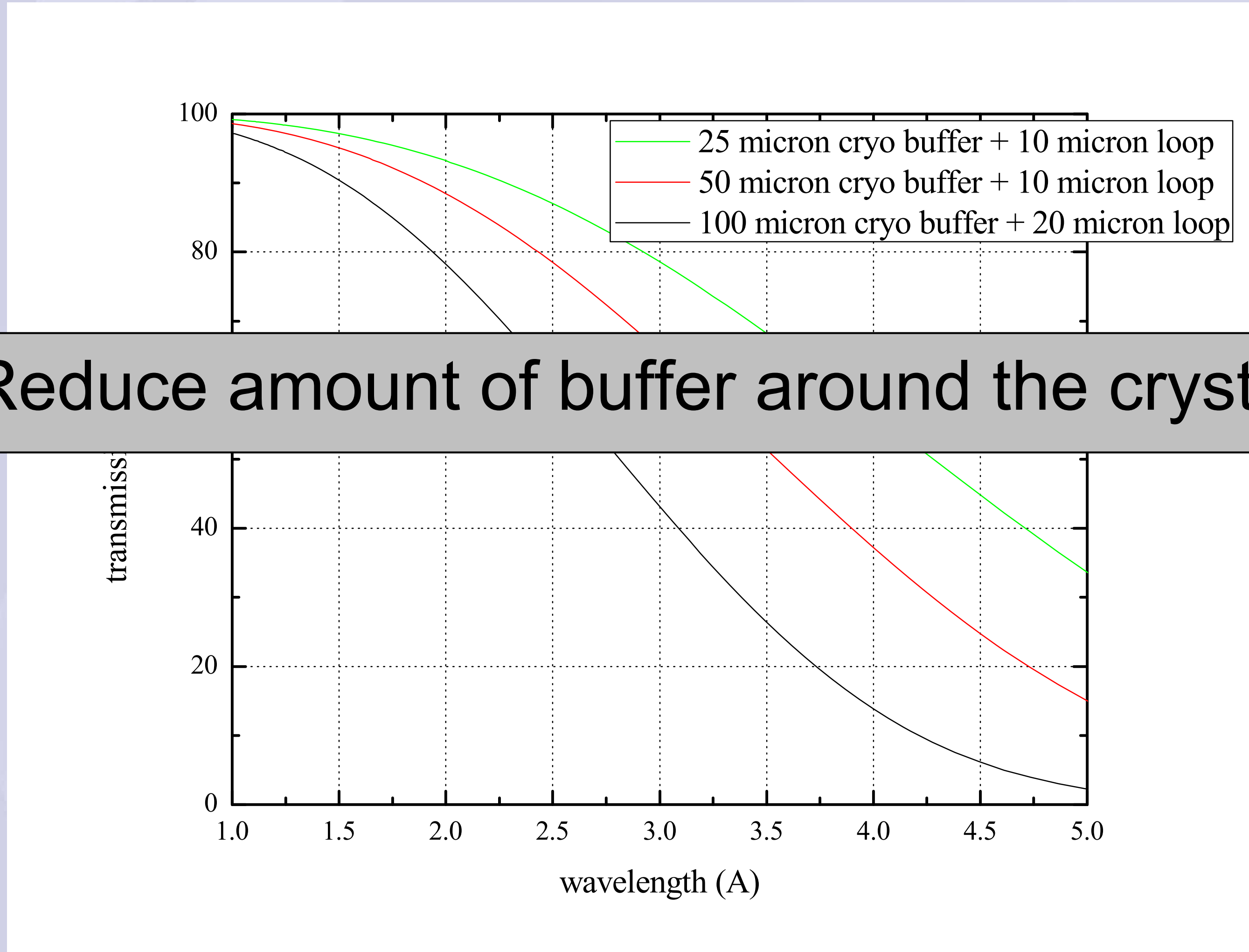

Reduce amount of buffer around the crystal!

diamond

I23 – Long wavelength MX beamline

Energy (wavelength) range:

2.1 - 12 keV (1 - 5.9 Å), optimized for 3 - 8 keV (1.5 - 4 Å)

Band-pass (ΔE/E):

2×10^{-4}

Beam size at sample:

100 - 1000 μm

Photon flux:

5×10^{12} ph/s in 100 x 100 μm @ 4 keV

End station:

Multi-axis goniometer in vacuum with micrometer precision for X-ray diffraction and tomography experiments from frozen macromolecular crystals in the temperature range 30 - 120 K.

Detector:

Area detector with high quantum efficiency to cover large solid angle


B23
B22
I23

Beamline Layout

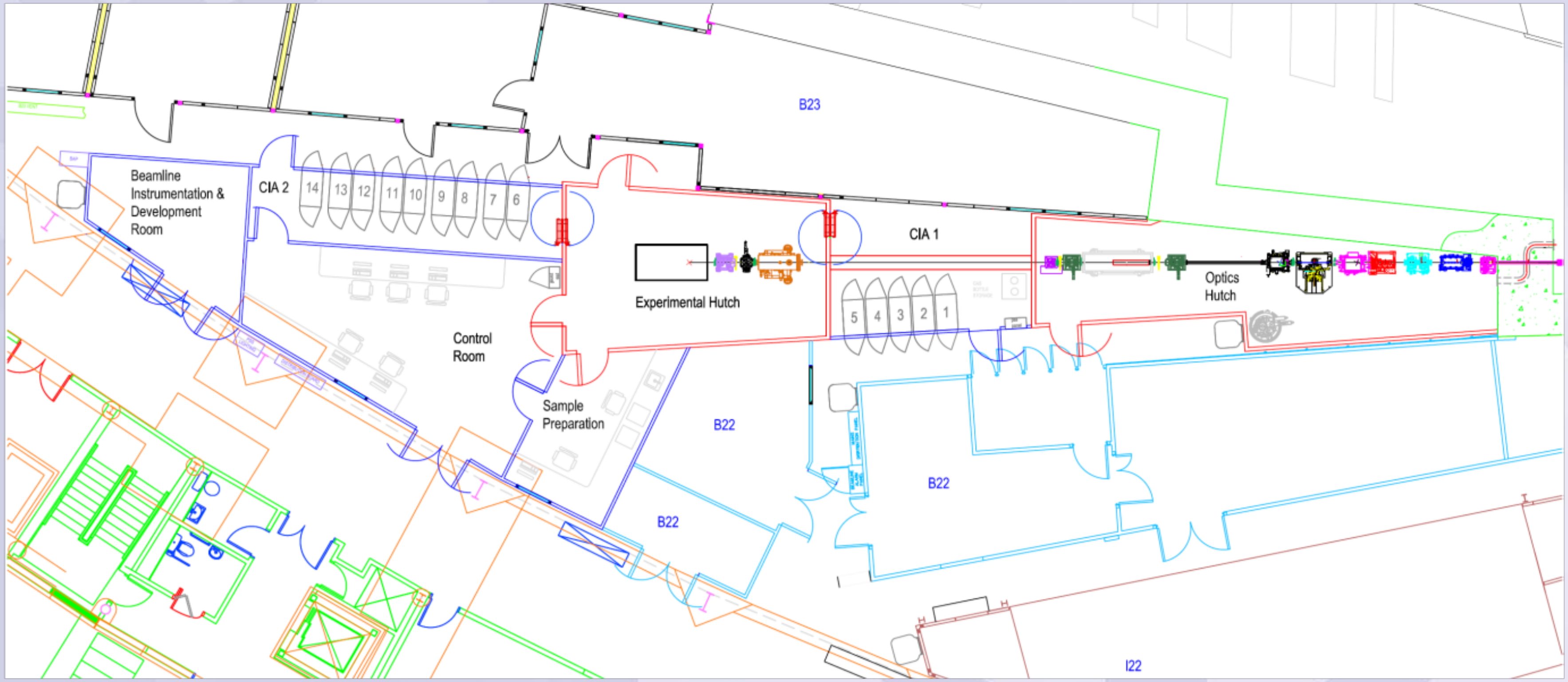

Insertion Device Front End

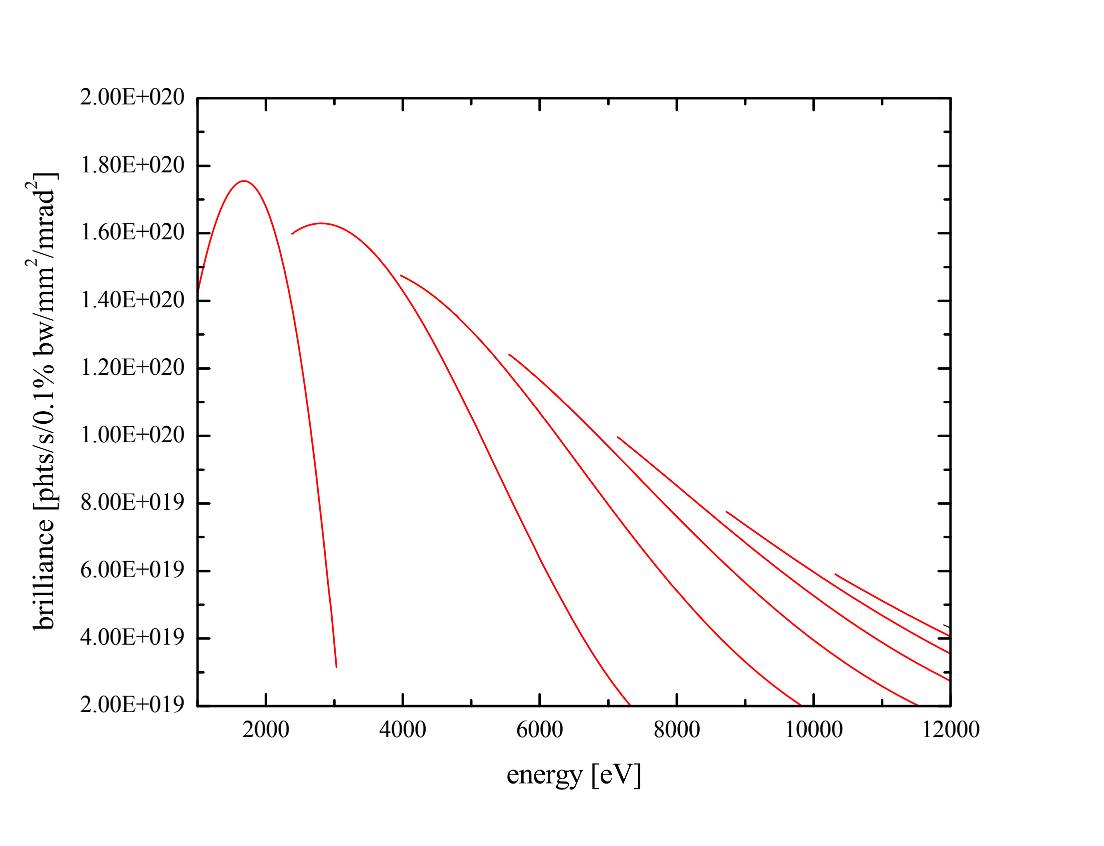

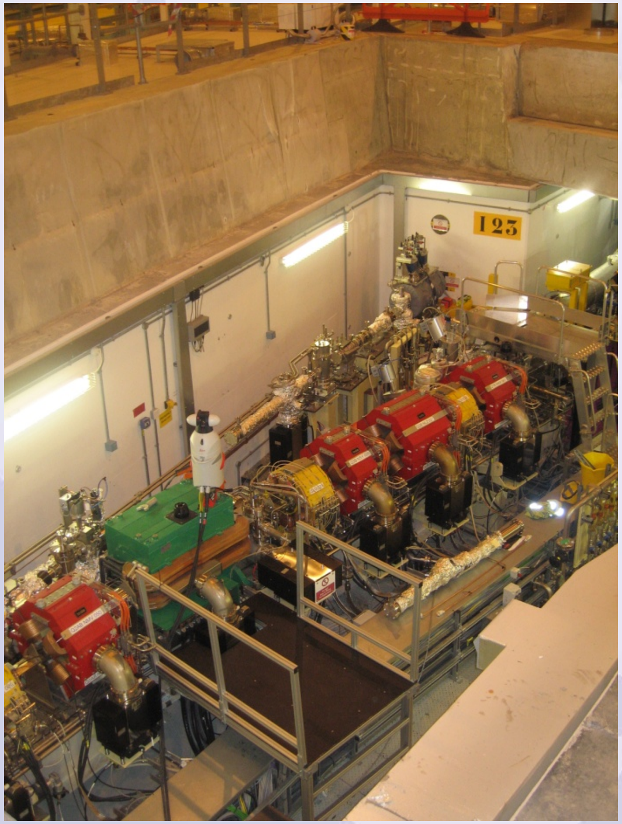

Phase I of FE installation during Christmas shutdown.

Optical layout

- All mirrors horizontally deflecting.
- Elliptical mirror for tangential focussing in horizontal plane.
- Cylindrical mirror for sagittal focussing in vertical plane.
- Two flat mirrors for harmonic rejection.

- Fast switching by moving first and last mirror either vertically or horizontally out of the beam.
- No optical elements for tomography!

Four-mirror system (case A)

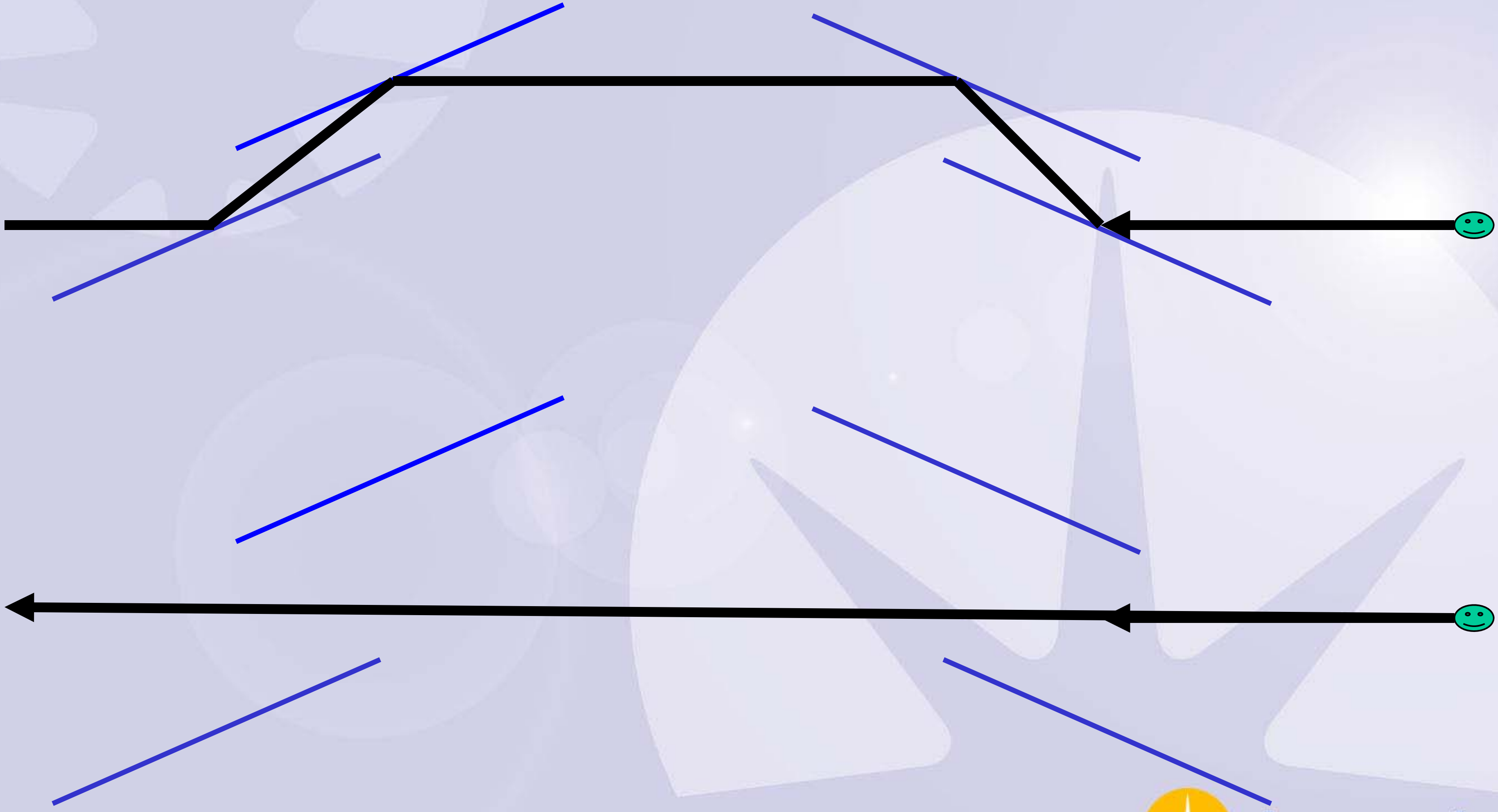

No optical elements, no harmonic rejection for tomography

Four-mirror system (case B)

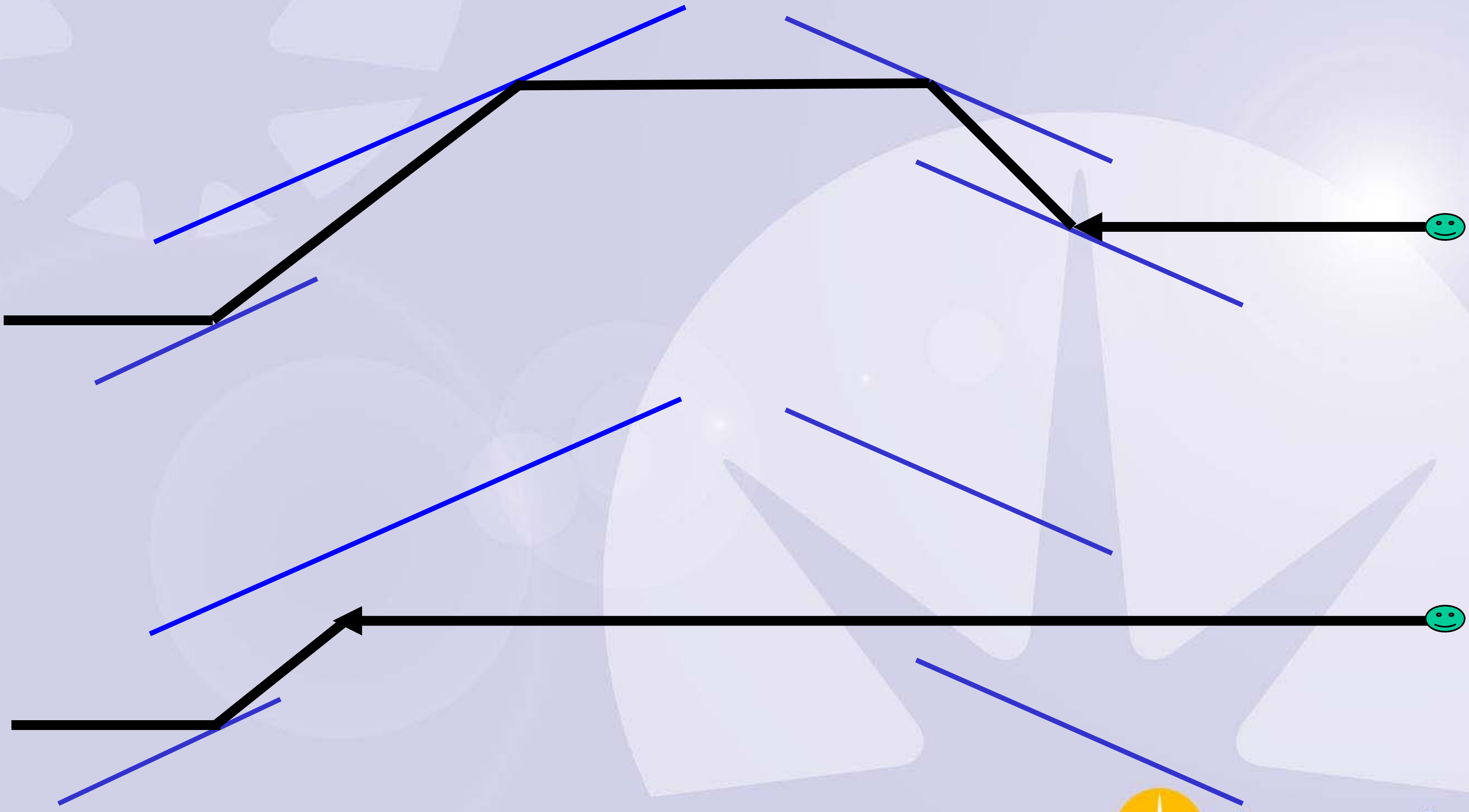

Two mirrors for harmonic rejection for tomography

Challenges

- Absorption
- Limited resolution
- Radiation damage

Air absorption

    Vacuum sample environment

Crystal, solvent and loop absorption

    X-ray tomography

    Analytical absorption correction

diamond

Conductive sample cooling

- As one main risk the User Working Group identified the efficiency of conductive cooling for protein crystals.

- Main uncertainty, thermal contact conductance to allow sample change and conductivity of vitreous ice.

diamond

Thermal conductivity of vitreous ice

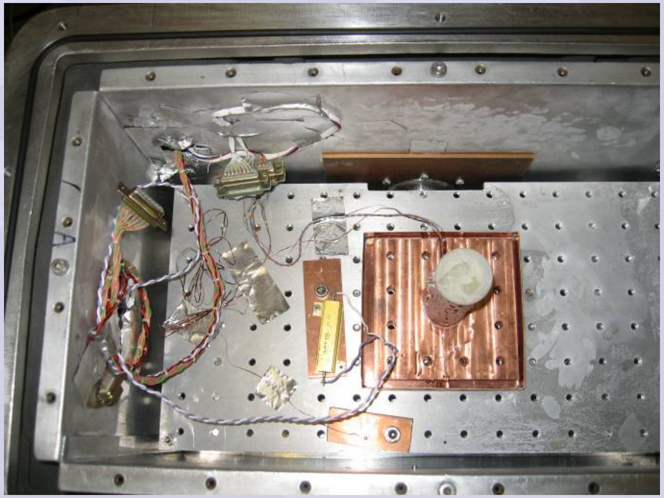

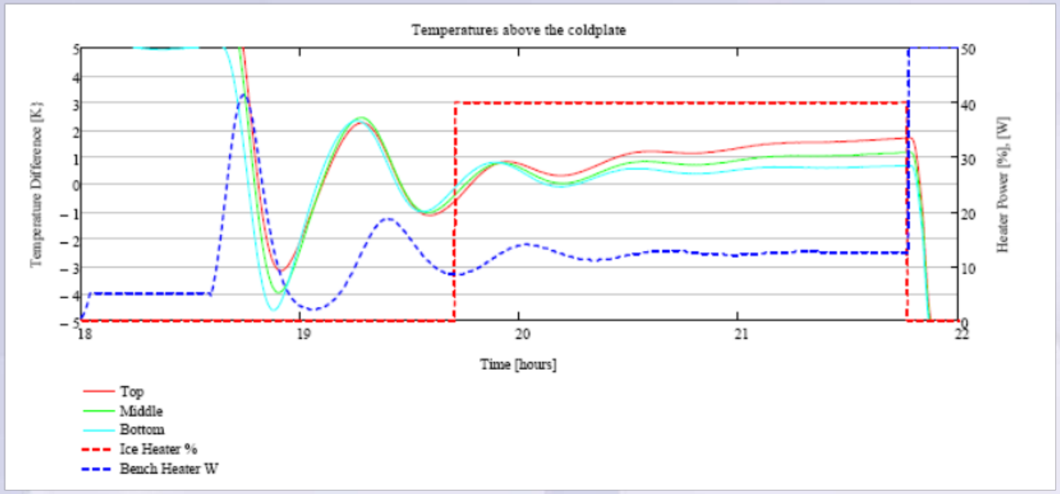

- Preliminary results
  - 3.5 $Wm^{-1}K^{-1}$ from temperature differences between sensors in vitreous ice sample (20% Ethylenglycol)
  - 1.9 $Wm^{-1}K^{-1}$ from cooling rate

Crystal Heating

- 20 MGy in 30 s
- Cylindrical crystal 100 μm long, 30 μm diameter
- Protein crystal density (30% solvent)
- 0.059 mW on crystal

Diamond ice crystal

- Thermal conductivity of crystal like vitreous ice

- Heating: <5 K

Sample transfer

EM VCT100 shuttle with specimen and holder

EM VCT100 cryo preparation workstation

- Standard system without customization

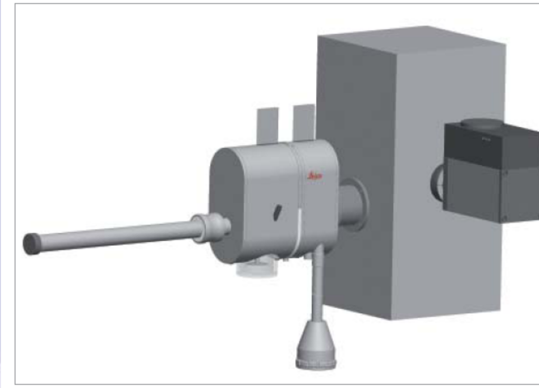

EM VCT100 docking station and shuttle with specimen and holder connected to the cryo stage.

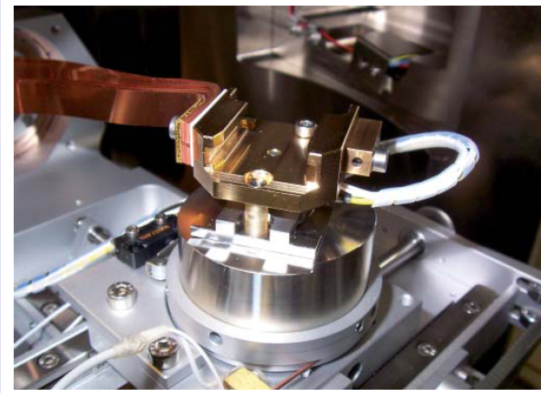

Custom-made cryo stage

The EM VCT100 is compatible with all current SEMs.

X-ray Tomography

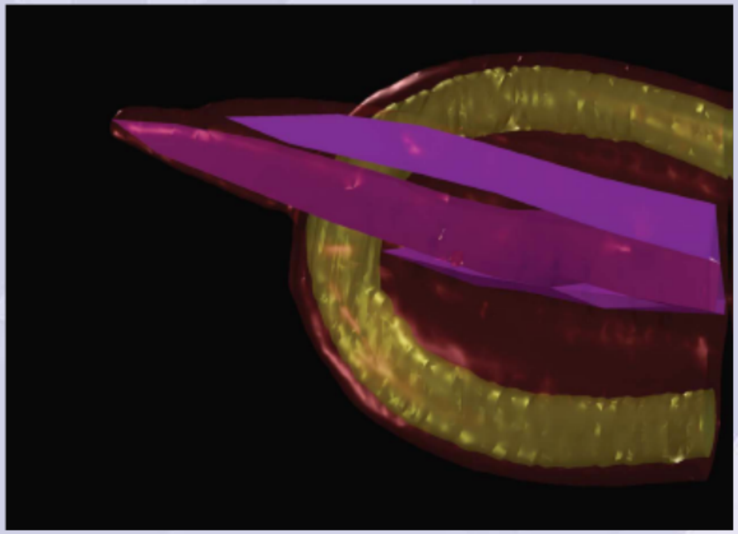

- Both absorption and phase contrast can be exploited
- Resolution: ~1 μm
- Diamond software development for analytical absorption correction based on tomographic reconstruction

Brockhauser et al. J. Appl. Cryst. (2008) 41, 1057.

Diamond Developments

Analytical absorption correction based on tomographic reconstructions

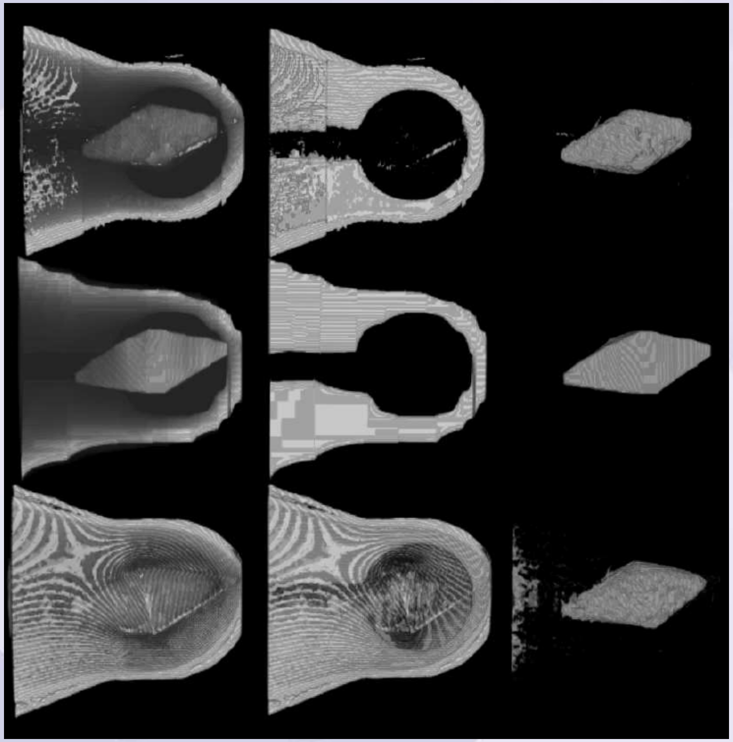

W. Armour et al.

3 publications in preparation.

Challenges

- Abs
- Lim
- Ra

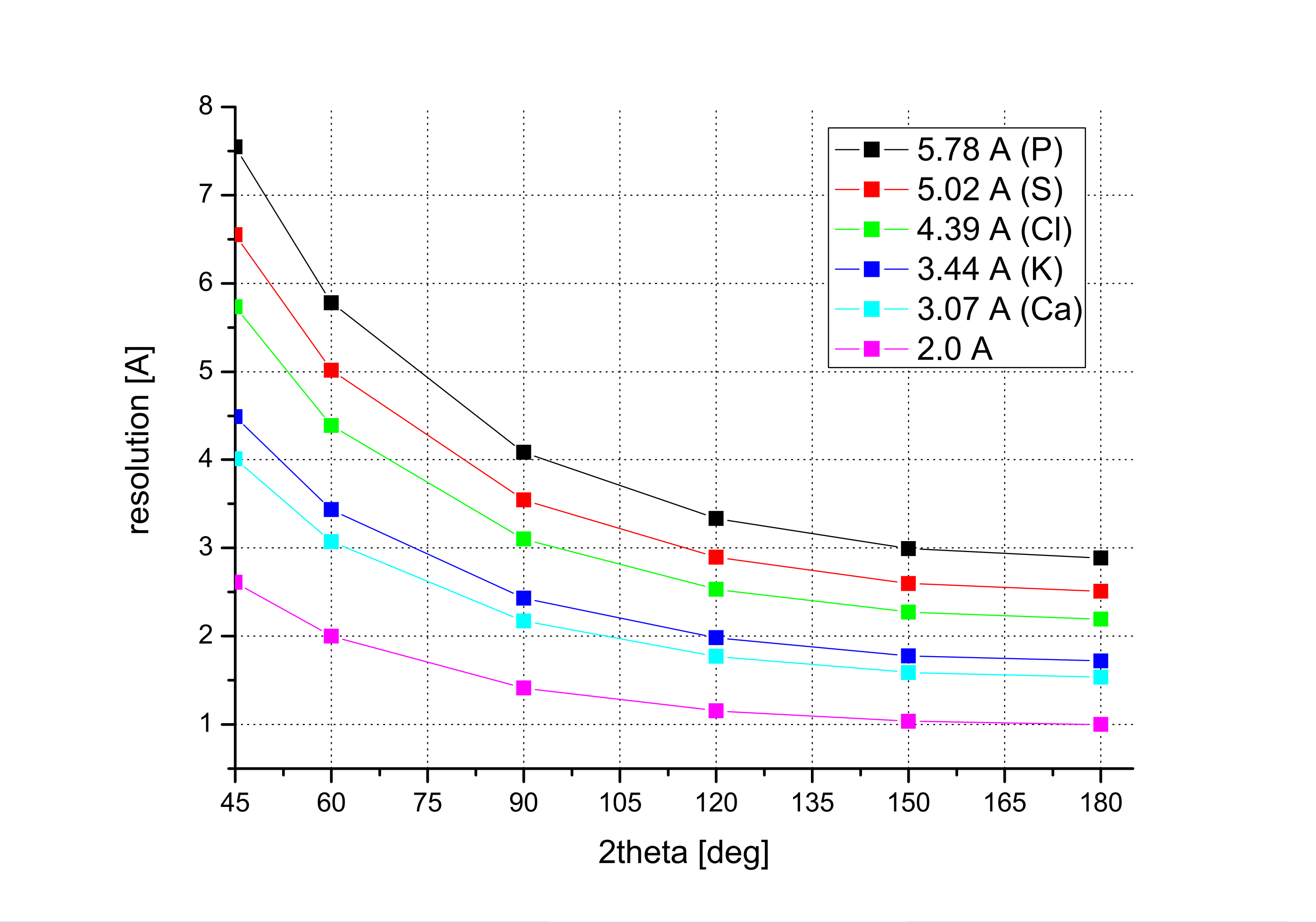

ion

tion

diamond

Detector

- Pilatus 6M
- Active area 431 x 448 mm^2
- Energy range 3–30 keV
- Readout time <3.6 ms
- Framing rate 10 Hz

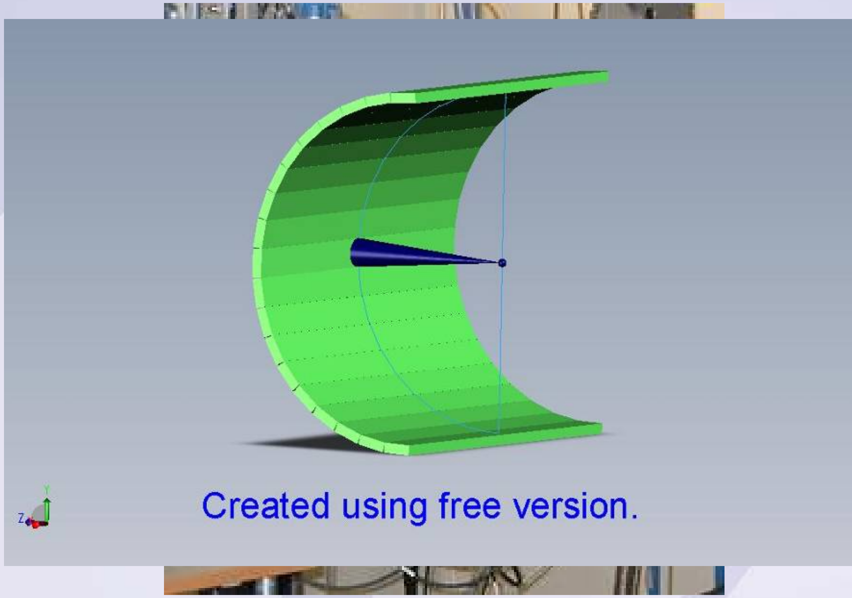

- No dark current
- No readout noise
- Single photon counter

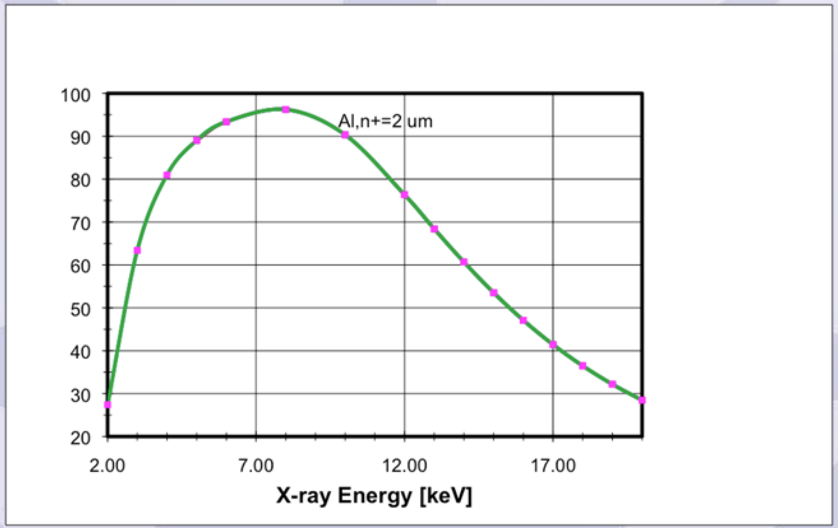

Detector

- Low-energy experiments on Diamond beamlines I18 and B16 to test Pilatus technology at low energies in vacuum.

Contents lists available at ScienceDirect

Nuclear Instruments and Methods in Physics Research A

journal homepage: www.elsevier.com/locate/nima

ELSEVIER

Performance of PILATUS detector technology for long-wavelength macromolecular crystallography

J. Marchal *, A. Wagner

Diamond Light Source Ltd, Harwell Science and Innovation Campus, Didcot, Oxfordshire OX11 0DE, UK

ARTICLE INFO

Keywords:
Pixel detector
Crystallography
X-ray diffraction
Synchrotron

ABSTRACT

The long-wavelength MX beamline I23 currently under design at Diamond Light Source will be optimized in the X-ray energy range between 3 and 5 keV. At the moment no commercial off-the-shelf detector with high quantum efficiency and dynamic range is available to cover the large area required for diffraction experiments in this energy range. The hybrid pixel detector technology used in PILATUS detectors could overcome these limitations as the modular design could allow a large coverage in reciprocal space and high detection efficiency. Experiments were carried out on the Microfocus Spectroscopy beamline I18 at Diamond Light Source to test the performance of a 100K PILATUS module in the low-energy range from 2.3 to 3.7 keV.

JINST

PUBLISHED BY IOP PUBLISHING FOR SISSA

RECEIVED: *September 15, 2011*
ACCEPTED: *November 9, 2011*
PUBLISHED: *November 30, 2011*

13th INTERNATIONAL WORKSHOP ON RADIATION IMAGING DETECTORS,
3–7 JULY 2011,
ETH ZURICH, SWITZERLAND

Low-energy X-ray detection with an in-vacuum PILATUS detector

Julien Marchal,[a,1] Benjamin Luethi,[b] Catalin Ursachi,[a] Vitaliy Mykhaylyk[a] and Armin Wagner[a]

[a]*Diamond Light Source,*
Harwell Science and Innovation Campus, Didcot, Oxfordshire, OX11 0DE, U.K.
[b]*Dectris Ltd,*
Neuenhoferstrasse 107, 5400 Baden, Switzerland

diamond

Pilatus 12M

- In-vacuum detector
- Half cylinder r = 250 mm
- $2\theta = \pm 90^{o}$

diamond

Royal Observatory Edinburgh

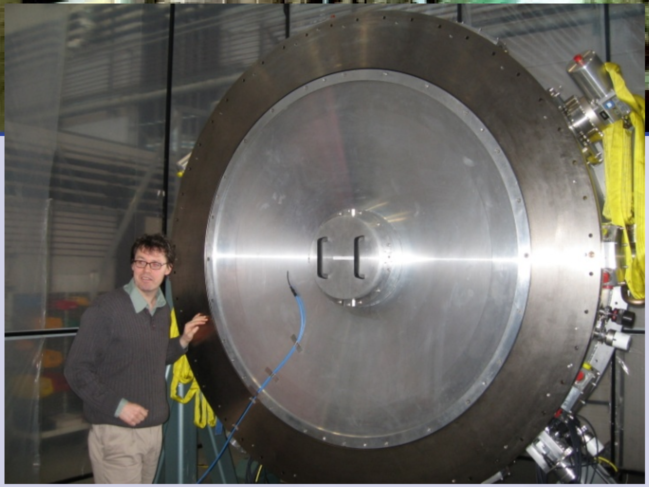

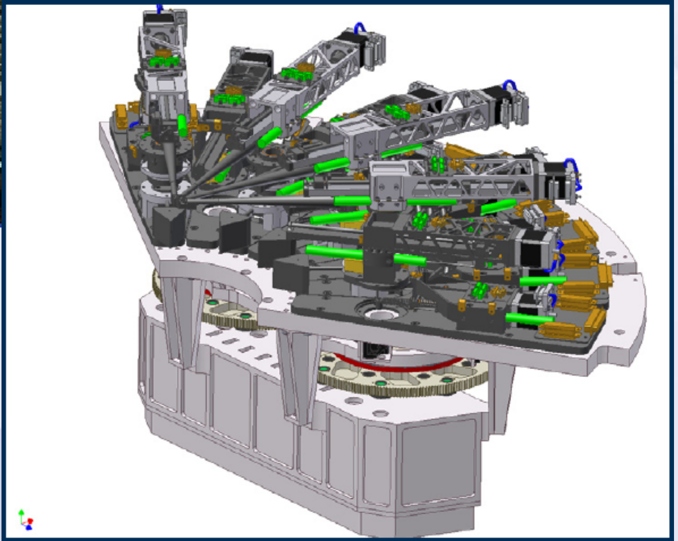

A section of the instrument showing the pick off arms and calibrator.

KMOS K-band multi-object spectrometer

To be installed at European Southern Observatory in Chile soon.

diamond

In-vacuum goniometer

- Commissioned to Astronomy Technology Centre in Edinburgh
- 3 μm sphere of confusion

diamond

Challenges

- Absorption
- Limited resolution
- Radiation damage

Air absorption

    Vacuum sample environment

Crystal, solvent and loop absorption

    X-ray tomography
    Analytical absorption correction

    Large area detector
    2theta arm
    Multi axis goniometer

diamond

Radiation Damage

- Most severe limitation on 3rd generation synchrotrons
- Drastic reduction from RT to 100 K
- 95% of experiments at 100 K
- Specific radiation damage alters anomalous substructure

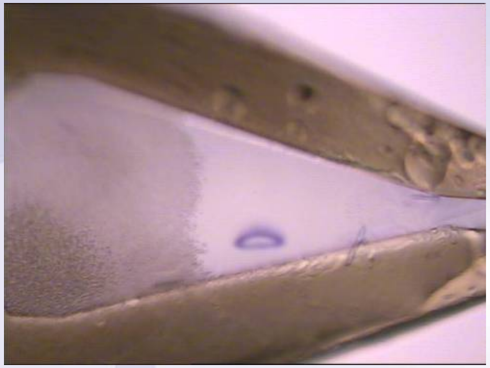

10 s exposure
(protein buffer + 20% ethylenglycol)

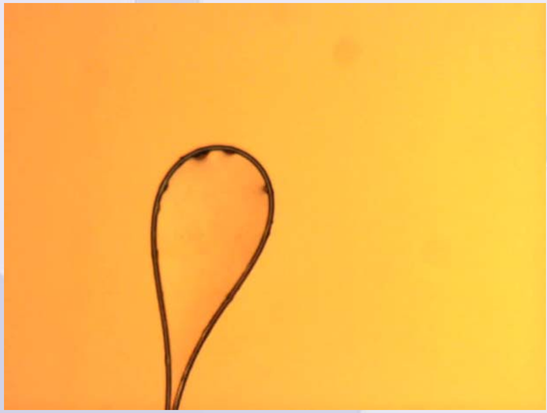

200 s exposure (30% ethylenglycol)
Warming up to ~200K

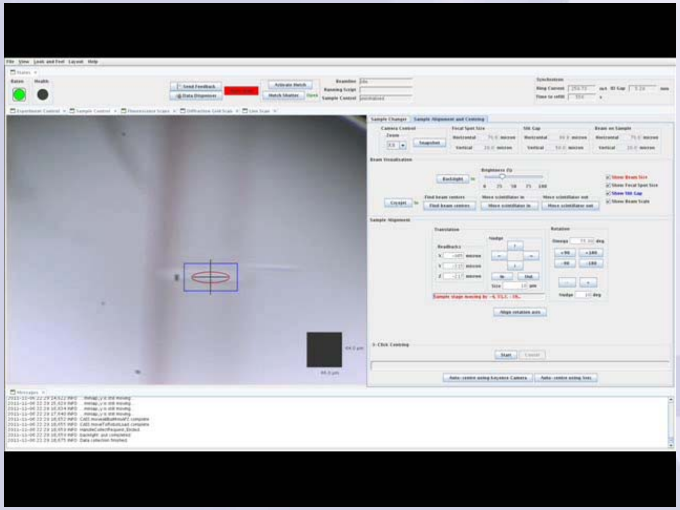

diamond

Specific radiation damage

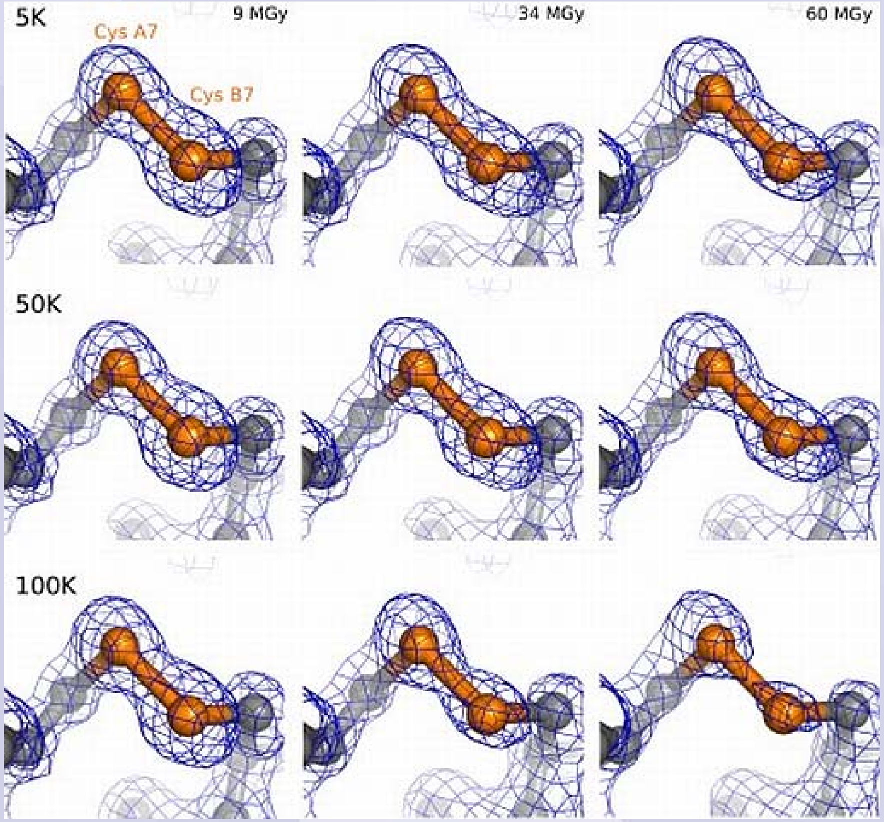

- A. Meents, S. Gutmann, A. Wagner, C. Schulze-Briese (2010) PNAS 107, 1094 – 1099.

Summary

End station most important aspect of beamline!

- High precision in-vacuum multi-axis goniometer
- In-vacuum detector
- Conductive cooling for temperatures ~40 K
- Sample holders compatible with cooling
- Sample transfer of frozen crystals into vacuum chamber
- Integration of tomography system

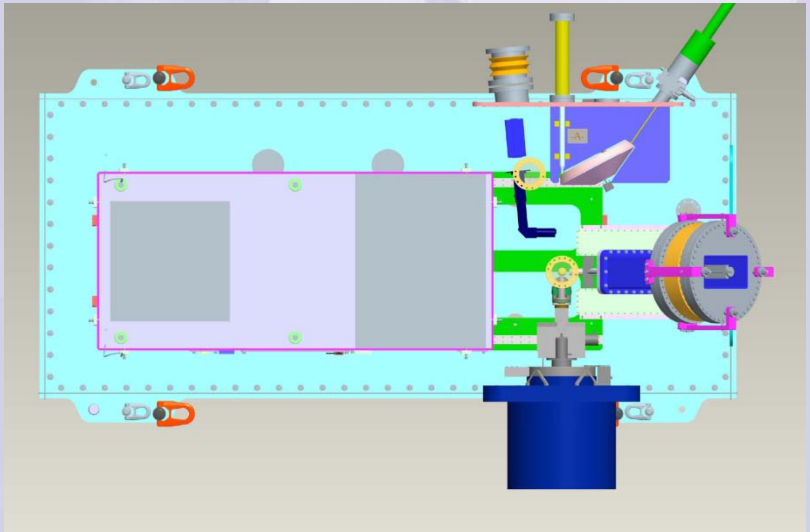

diamond

Milestones	Date
Design	
Conceptual Design Report Review	12/01/09
Technical Design Report Review	01/07/10
Construction	
Hutches Complete	19/07/11
Hutches, Cabins and Services complete	27/03/12
Installation	
Optics Hutch installation complete	04/09/12
Experimental Hutch installation complete	10/04/13
Commissioning	
First Light for beamline I23	06/09/12
I23 First User	04/10/13

diamond

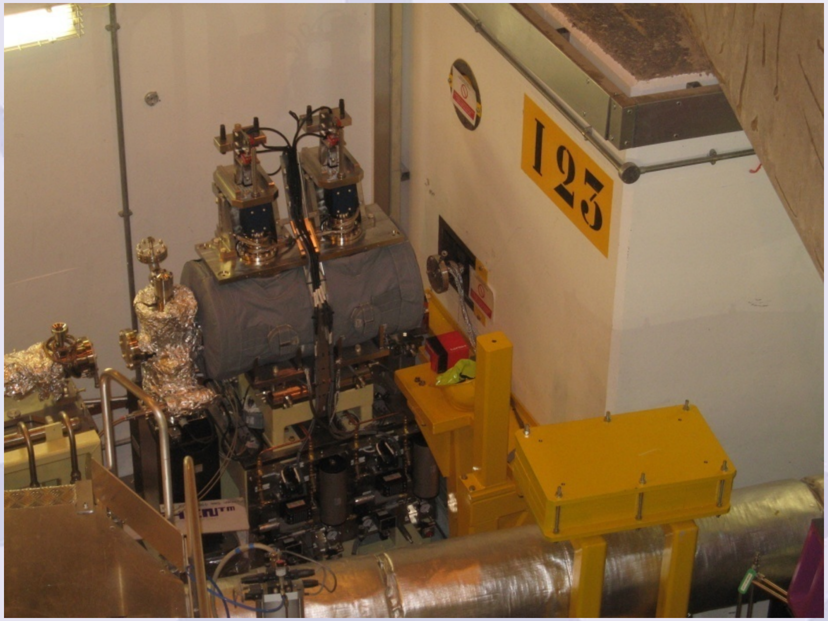
I23

Project Team

- Vitaliy Mykhaylyk (Beamline scientist)
- Martin Burt (Project engineer)
- Jon Kelly (Mechanical engineer)
- Kevin Wilkinson (Electrical engineer)
- Gary McIntyre (Design engineer)
- Stephen Green (Design engineer)
- Ronaldo Mercado (Controls)
- Richard Fearn (Data Acquisition)
- Lucia Alianelli (Optics)
- Emily Longhi (ID)
- Julien Marchal (Detectors)